Front. Med. 2024, 18(1): 68−80
https://doi.org/10.1007/s11684-023-1005-y

RESEARCH ARTICLE

Association of *TRMT2B* gene variants with juvenile amyotrophic lateral sclerosis

Yanling Liu[1,2,*], Xi He[3,*], Yanchun Yuan[4], Bin Li[4,5,6], Zhen Liu[4], Wanzhen Li[4], Kaixuan Li[2], Shuo Tan[2], Quan Zhu[2], Zhengyan Tang[2], Feng Han[2], Ziqiang Wu[2], Lu Shen[4,5,6,7,8,9], Hong Jiang[4,5,6,7], Beisha Tang[4,5,6,7], Jian Qiu[5,6,7,10], Zhengmao Hu (✉)[7,*], Junling Wang (✉)[1,4,5,6,7,8,9,*]

[1]*Department of Neurology, Xiangya Hospital, Central South University, Jiangxi, National Regional Center for Neurological Diseases, Nanchang 330038, China;* [2]*Provincial Laboratory for Diagnosis and Treatment of Genitourinary System Disease, Department of Urology, Xiangya Hospital, Central South University, Changsha 410078, China;* [3]*Department of Orthopedics, The First Affiliated Hospital, Zhejiang University School of Medicine, Hangzhou 310002, China;* [4]*Department of Neurology, Xiangya Hospital, Central South University, Changsha 410078, China;* [5]*National Clinical Research Center for Geriatric Diseases, Xiangya Hospital, Central South University, Changsha 410008, China;* [6]*Key Laboratory of Hunan Province in Neurodegenerative Disorders, Central South University, Changsha 410008, China;* [7]*Center for Medical Genetics, School of Life Sciences, Central South University, Changsha 410008, China;* [8]*Engineering Research Center of Hunan Province in Cognitive Impairment Disorders, Central South University, Changsha 410078, China;* [9]*Hunan International Scientific and Technological Cooperation Base of Neurodegenerative and Neurogenetic Diseases, Changsha 410078, China;* [10]*Hunan Key Laboratory of Molecular Precision Medicine, Xiangya Hospital, Central South University, Changsha 410078, China*

Abstract **Amyotrophic lateral sclerosis (ALS) is a fatal neurodegenerative disease characterized by progressive degeneration of motor neurons, and it demonstrates high clinical heterogeneity and complex genetic architecture. A variation within *TRMT2B* (c.1356G>T; p.K452N) was identified to be associated with ALS in a family comprising two patients with juvenile ALS (JALS). Two missense variations and one splicing variation were identified in 10 patients with ALS in a cohort with 910 patients with ALS, and three more variants were identified in a public ALS database including 3317 patients with ALS. A decreased number of mitochondria, swollen mitochondria, lower expression of ND1, decreased mitochondrial complex I activities, lower mitochondrial aerobic respiration, and a high level of ROS were observed functionally in patient-originated lymphoblastoid cell lines and *TRMT2B* interfering HEK293 cells. Further, *TRMT2B* variations overexpression cells also displayed decreased ND1. In conclusion, a novel JALS-associated gene called *TRMT2B* was identified, thus broadening the clinical and genetic spectrum of ALS.**

Keywords *TRMT2B*; amyotrophic lateral sclerosis; mitochondrial complex I; tRNA methylation; reactive oxygen species

Introduction

Amyotrophic lateral sclerosis (ALS) is a devastating neurodegenerative disease characterized by progressive degeneration of upper and lower motor neurons, leading to muscular weakness and atrophy [1]. The incidence of ALS varies among different populations, ranging from 0.8–1.2 to 2.1–3.8 per 100 000 person–years in China and Europe, respectively [2]. Accumulating evidence indicates that genetic background, environmental exposure, and aging are risk factors implicated in the pathogenesis of ALS [3,4]. Genetically, approximately 10% of ALS cases are familial, and over 40 genes have been directly linked to ALS through next-generation sequencing [5]. In China, *SOD1* has been identified as the most frequent ALS pathogenic gene, followed by *TARDBP* and *FUS* [6].

ALS typically occurs in individuals aged between 42 and 65 years, invariably leading to death due to respiratory failure 3–4 years after the onset [1,7]. Juvenile ALS (JALS), a rare form of ALS, is defined as age at onset less than 25 years [8]. Some patients of familial ALS (fALS) subtypes, such as ALS2, ALS4, ALS5, ALS6, and ALS16, are juvenile-onset, and most of these cases are inherited as an autosomal recessive pattern.

Received December 4, 2022; accepted April 27, 2023

Correspondence: Junling Wang, junling.wang@csu.edu.cn;
Zhengmao Hu, huzhengmao@sklmg.edu.cn

*These authors contributed equally to this work.

JALS is more frequently recognized to have a genetic origin than adult-onset ALS, suggesting that studies on JALS may provide an opportunity to identify more novel causative genes [8]. Till now, several genes, including *SPTLC1* [9], *FUS* [10], *ALS2* [11], *SETX* [12], *SPG11* [13], and *SIGMAR1* [14] have been identified in JALS. These disease causative genes underlying JALS also play a role in adult-onset ALS [9]. The identification of these genes contributed to disclosing the molecular mechanisms underlying ALS. However, the etiology is not fully illustrated, and further genetic research may discover novel disease-associated genes and provide new clues to the disease pathogenesis.

Mitochondrial malfunctions play a pivotal role in the development of ALS [15–17]. The mitochondria produce energy for cellular biochemical reactions, which are essential for the survival of motor neurons and are implicated in the process of generating reactive oxygen species (ROS). The changes occurring in the mitochondrial respiratory chain enzymes have been implicated in ALS pathophysiology [18]. Haploinsufficiency of *C9ORF72*, an ALS pathogenic gene, causes impairment of respiratory complex I assembly in patients with ALS [19].

In this study, a novel ALS-associated gene, *TRMT2B*, was identified in a JALS family, and additional *TRMT2B* variants were discovered in large cohorts of patients with ALS. Functional analysis revealed that *TRMT2B* may participate in the pathogenesis of ALS by impairing the functional activity of the mitochondria.

Materials and methods

Patients and clinical analysis

A family (XY003) that included two members who had ALS was recruited in Hunan Province, China (Fig. 1A). The two patients and their one unaffected sister and

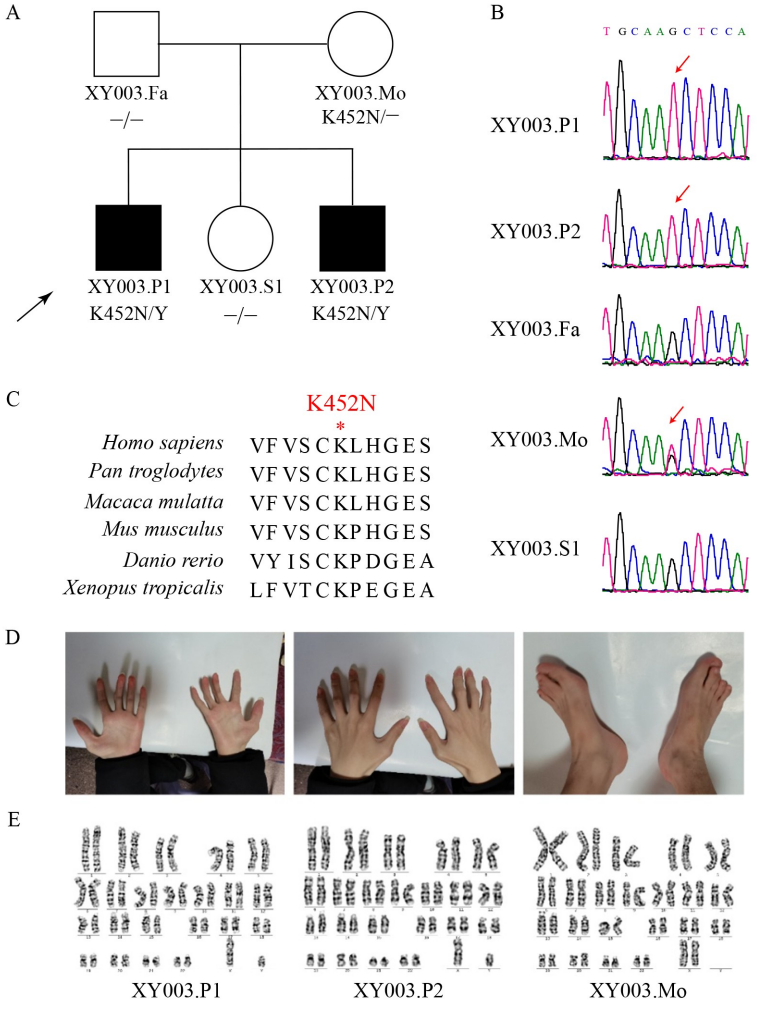

Fig. 1 *TRMT2B* was identified to be associated with ALS in a JALS family. (A) JALS family recruited from Hunan, China. The black arrow indicated the proband. (B) *TRMT2B* c.1356G > T; p.K452N variant co-segregated in this family. (C) Highly conserved K452 on TRMT2B protein among species. (D) Patient deformity of hands and feet. (E) Karyotypes of patients and their mother.

parents underwent full physical and clinical examinations, including electromyography, electrocardiography, brain magnetic resonance imaging (MRI), cognitive function evaluation, and blood biochemistry tests.

In this study, 910 cases with ALS from China were enrolled for mutation screening of the candidate genes [20]. This ALS cohort included 753 patients with ALS, which were reported previously [7]. Among these patients, pathogenic polynucleotide expansions in *C9ORF72* and *ATXN2* were excluded. The patients' demographic characteristics are listed in Table 1. *TRMT2B* gene variants were also analyzed in an independent publicly available ALS cohort (ALSdb) comprising 3317 sporadic ALS cases subjected to whole-exome sequencing (WES). For controls, 104 068 exomes of non-neuro individuals in the gnomAD version 2 database were analyzed. The ALS-associated genes excluded for all patients are shown in Table S1.

Table 1 Demographic characteristics of patients with ALS

	ALS cohort
No. of patients with ALS	910
Juvenile ALS	14
Family history (number)	68
Male (number, rate%)	597, 65.5%
Age at onset (years)	53.75 ± 11.28

This study was approved by the Ethics Committee of Xiangya Hospital, Central South University, China, under approval number 202103191. All participants provided written informed consent to participate in the study.

Karyotype analysis and whole-genome genotyping

Karyotype analysis was performed on peripheral blood lymphocytes by using the G-banding method as described before [21]. Genomic DNA was extracted from the peripheral blood of all participants [22]. Whole-genome genotyping was performed using an Illumina ASA 750K Chip. Genotype analysis was carried out using the Illumina GenomeStudio Genotyping Module (version 2011.1). The CNV gap value was set as 100 M.

WES

Samples of the two patients and their unaffected parents were subjected to WES as previously described [7,23]. Different filtering pipelines were used as the disease may be inherited by the family in an X-linked or autosomal recessive pattern. Rare damage variants (RDVs) that fulfilled the following criteria were included for further analysis: (1) rarity: heterozygous variants with a minor allele frequency (MAF) of less than 0.1% in the 1000 Genome Project and gnomAD; (2) nonsynonymous substitutions, indels, and putative splice site variants; (3) variant pathogenicity predicted by at least two of 11 *in-silico* tools; (4) for the X-linked pattern, all consensus variations in the X chromosome were extracted from both patients in the family, and for the autosomal recessive inheritance pattern, all consensus homozygous or compound heterozygous variations were extracted from both patients in the family. The samples of the healthy sister and parents were included for co-segregation analysis.

Further screening of candidate variants was performed on the samples of the 910 patients with ALS in the cohort who underwent WES [7].

Mutant mRNA expression and qPCR

Lymphoblastoid cells were isolated from blood samples and immortalized using the Epstein–Barr virus [22]. Total RNA was extracted as described before [22]. PCR was performed with primers TRMT2B-F/R (Table S2) by using Premix (Takara). The amplified product was inserted into the T-vector (Takara) and sequenced. qPCR was performed with actin and ND1 primers (Table S2) by using TB Green Premix (Takara) on QuantStudio (Invitrogen).

Plasmid construction and cell transfection

TRMT2B cDNA (NM_001167972.2) was amplified by PCR using primers TRM-F/R (Table S2). Premix (Takara) was used to amplify the target sequence and inserted into the PCDNA3.1(+) plasmid by using T4 ligase (Thermo Scientific). The mutated *TRMT2B* cDNA was amplified using specific primers (Table S2) and cloned as described above. HEK293 cells were transfected with jetPRIME in accordance with the manufacturer's instructions.

Gene interfering

TRMT2B siRNA with target sequence of 5′-CTGGTCA AGCAGAGAAGATTT-3′ and 5′-GCACAGTATGTAA GGGAGATT-3′ was purchased from Sangon. HEK293 cells were transfected with jetPRIME in accordance with the manufacturer's instructions. RNAi lentivirus particles, with identical target sequences, were purchased from Genechem. Samples were tested 14 days after the lentivirus infection.

Immunoblotting and immunofluorescence

For immunoblotting, the lymphoblastoid cells from the patients and normal participants were lysed in RIPA buffer. Protein electrophoresis was conducted as described before [22]. The expression of TRMT2B and

p62 was analyzed using antibodies. Anti-β-actin antibodies were used for loading control.

For immunofluorescence, HEK293 cells cultured in DMEM with 10% FBS (Invitrogen) were plated on collagen-coated coverslips and fixed with 4% ice-cold paraformaldehyde. The procedures of immunofluorescence were identical as described before [24]. Images were analyzed by confocal microscopy (Zeiss). The antibodies used in this study are listed in Table S3. Co-localization analysis was performed using the ImageJ plugin colocalization-finder.

Activities of mitochondrial complexes I and III

In each sample, 5×10^6 lymphoblastoid cells were used for mitochondrial extraction. The activity of mitochondrial complex I was assessed by the NADH oxidation rate measured on the basis of absorbance at 340 nm. The activity of mitochondrial complex III was assessed by the rate of cytochrome C increase on the basis of absorbance at 550 nm. The assays on mitochondrial complexes I and III were performed using the mitochondrial complexes I and III activity kits, respectively (Solarbio).

Mitochondrial aerobic respiration

In each sample, 10^5 cells were seeded on a seahorse assay plate and cultured overnight. The medium was then replaced with the Seahorse XF base medium, and the cells were incubated in a 37 °C incubator without CO_2 for 1 h. After the baseline oxygen consumption rate (OCR) was measured, oligomycin (1 μmol/L, complex V inhibitor), carbonyl cyanide 4-(trifluoromethoxy) phenylhydrazone (FCCP, 2 μmol/L, uncoupler), and rotenone/antimycin A (0.5 μmol/L each, complexes I and III inhibitors) were added sequentially. The OCR measurements, including basal, maximum respiration, spare-respiratory capacity, ATP synthesis, proton leak, and non-mitochondrial respiration, were obtained and calculated as previously described [25]. The OCR values were normalized to the sample protein concentration.

Flow cytometry detection of ROS

Cells were incubated with dihydroethidium (Applygen) diluted in PBS (1:1000) for 30 min at 37 °C, washed in PBS three times to remove the residual probe, and analyzed by flow cytometry using FACSCanto II (BD). The data were evaluated using the FlowJo software.

Transmission electron microscopy (TEM)

Cells were incubated in iced 2.5% glutaraldehyde solution for 1 h and then washed with iced PB buffer five times. Next, 2% osmic acid was added to each sample, and the samples were washed with iced ddH_2O five times. They were then replaced with ethanol and embedded with SPI-Pon 812. Leica EM UC7 ultramicrotome was used to obtain 70 nm slices, and classical staining with 2% uranyl acetate and lead citrate was performed. All the TEM images were captured using Hitachi 7700.

Statistical analysis

Statistical analysis was performed using SPSS 25.0. Association analysis of RDVs across *TRMT2B* was performed in the ALS cohort by using Fisher's exact test for each allele. An unpaired *t*-test was conducted using Prism. A *P* value of 0.05 indicated statistical significance.

Data availability statement

The datasets analyzed in this study are not publicly available. Further information about these datasets is available from the senior authors (Jungling Wang and Zhengmao Hu) upon reasonable request.

Results

Clinical characteristics of patients with JALS

The proband of the XY003 family (Fig. 1A) was a patient in his 30s who initially developed weakness of the lower limbs at childhood age. Before the age of 10 years, weakness of the upper limbs occurred. The patient also showed delayed cognitive and motor developmental milestones, and his school performance was worse than average. At the age of 20s, he suffered from a decrease in visual acuity of the left eye. He complained of progressive exacerbation of limb weakness but not of dysphagia or dysarthria. A detailed medical record was not available. On admission, the patient had a small stature, which was below the genetic expectation, and deformity of hands and feet (Fig. S1A–S1C). He also showed low activity endurance and ability to exercise. A neurological examination revealed obvious muscle weakness and atrophy of the four extremities, facial muscle bundle tremor, and normal eye movement but incomplete eye closure. Furthermore, the proband showed a slight increase in muscle tension in the lower limbs and stiffness of ankle joints, which induced ankle clonus. He also showed cognitive decline (executive dysfunction and memory impairment). The proband's younger brother (XY003.P2) showed the same lower limb weakness at childhood age and similar symptoms at the age of 20s (Figs. 1D and S1D–S1F). The detailed clinical information is described in Table 2. Their sister and parents had no neurological symptoms or signs.

Nerve conduction studies revealed an obvious reduction

Table 2 Clinical features of patients with JALS carrying TRMT2B variants

Clinical feature	Patient 1	Patient 2
ID in family	XY003	XY003
Amino acid change	K452N	K452N
Sex	Male	Male
Age at onset (year)	< 5	< 5
Age at evaluation (year)	30s	20s
BMI	22.89	16.65
Hand deformities	Flexion contracture deformity	Flexion contracture deformity
Foot deformities	Pes cavus, hallux valgus, and ankle stiffness	Pes cavus and hallux valgus
Walking	Abnormal	Normal
Atrophy	Four extremities	Four extremities
Weakness	Generalized	Generalized
Reflexes	Normal	Normal
UMN signs	Ankle clonus and hypertonia	Hypertonia
Tongue	Fasciculations	NA
Jaw jerk	Present	Present
Dysarthria	Normal	Normal
Dysphagia	Normal	Normal
Respiratory	Normal	Normal
Cognition		
MMSE score	27/30	NA
ECAS score	68/136	NA
Sensory	Normal	Normal
Additional features	Visual damage	Visual damage and scapular winging
Neurophysiology		
Motor	Reduced CMAP, chronic neurogenic reinnervation, and ongoing denervation	Reduced CMAP, chronic neurogenic reinnervation, and ongoing denervation
Sensory	Normal	Normal

in compound action potential in the lower and upper limb nerves of the proband, but nerve conduction velocity (NCV) was normal. Meanwhile, sensory NCV studies did not detect any abnormalities. The electromyogram of the proband showed chronic neurogenic reinnervation, enlarged long-duration motor unit potentials in the cervical and lumbar spinal cord regions, and ongoing denervation (moderate spontaneous potentials in lower limb muscles). Chronic neurogenic reinnervation and ongoing denervation were not found in the sternocleidomastoid muscle. Left visual evoked potential (VEP) indicated an obvious reduction in the amplitude of the P100 component. The proband's younger brother also showed chronic neurogenic reinnervation in the cervical and lumbar regions and ongoing denervation in the thoracic region (moderate spontaneous potentials). He had the same VEP reduction as the proband. The proband and his younger brother had increased rest levels of creatine kinase (349 and 1099 U/L, respectively, vs. normal level of 50–310 U/L). In both patients, blood lactate was normal before exercise and slightly increased (less than twice) after exercise. The blood levels of ammonia, glucose, and lipids and thyroid function were normal. No obvious abnormalities were revealed by brain MRI (Fig. S2), ECG, and echocardiography.

Identification of *TRMT2B* variants associated with JALS

All coding and splice variants that were identified in the X chromosomes of the two affected patients were analyzed. After functional filtering, a hemizygous variation c.1356G>T (p.K452N, NM_001167972.2) was identified in *TRMT2B*. Sanger sequencing revealed segregation of the c.1356G>T mutation with the phenotypes in the XY003 family (Fig. 1B). The mother of the proband was heterozygous for this variant (Fig. 1B). The c.1356G>T mutation in *TRMT2B* has not been reported in 1000 Genomes Project or gnomAD databases, and it is highly conserved among species (Fig. 1C).

As *TRMT2B* is located on the X chromosome and the unaffected mother of the proband was a heterozygous carrier, TA cloning was conducted to determine the presence of the mutated *TRMT2B* mRNA in the lymphoblastoid cells of the mother. The results revealed only 8.5% (6/71) of mutant mRNA in the lymphoblastoid cells of the proband's mother, less than the expected rate of 50%.

The karyotypes of the patients and their mother were normal (Fig. 1E). CNV analysis on the two patients showed no consensus abnormities (Fig. S3). An analysis based on an autosomal recessive hereditary pattern was performed; however, only two genes fulfilling the analysis criteria were found, and none of them was associated with potentially neurodegenerative processes (Table S4).

Screening of *TRMT2B* variants in patients with ALS

The occurrence of *TRMT2B* variants in a cohort of 910 patients with ALS was evaluated to explore the variation role of *TRMT2B* in ALS. Among 10 patients, two missense variants (c.250C>G, L84V and c. 1344T>G, F448L) and one splice variant (c.539-3T>C) of *TRMT2B* were identified, which were rare or absent in gnomAD. Both missense variants were predicted to be damaging (Table 3 and Fig. S4). Notably, the L84V variant was identified in seven unrelated patients with sporadic ALS who had typical clinical features of adult-onset ALS without vision impairment. The mean age at onset was 57.22 ± 7.96 years (range of 42–66 years). A notable detail that three of the six patients who underwent cognitive tests had cognitive impairment (50%).

Among the 104 068 non-neuro individuals in the gnomAD version 2 database (47 831 females and 56 237 males), a total of 494 rare putative pathogenic *TRMT2B* variants from the WES data were identified in *TRMT2B* that fulfilled the same RDV analysis criteria. The results of gene burden testing revealed *TRMT2B* variations as a risk factor for the disease ($P = 0.003$ by Fisher's exact test). For variation L84V, the results of gene burden test showed significance in patients ($P < 0.0001$) compared with GnomAD. For variation F448L, the results of gene burden did not show significance in patients ($P = 0.0961$ by Fisher's exact test) compared with GnomAD or ExAC ($P > 0.99$ by Fisher's exact test). However, the results of gene burden showed significance in patients compared within GnomAD male section ($P = 0.0460$ by Fisher's exact test).

In an independent ALS cohort (ALSdb), three additional rare deleterious *TRMT2B* variants, namely, R334W (c.1000C>T), R315L (c.944G>T), and R162G (c.484C>G), were identified (Table 3 and Fig. S4). However, no clinical data were available online.

Patients with *TRMT2B* variations showed impaired mitochondrial function

Lymphoblastoid cell lines of the two patients and controls, including their heterozygous mother, the healthy sister of the XY003 family, and one unrelated man, were constructed. The unrelated man aged 24 years at the collection of the sample. He was mentally and physically healthy, and he received his master's degree 1 year after sample recruitment. He had no family history of neurodegeneration diseases, such as Alzheimer's disease (AD), Parkinson's disease, or ALS.

Compared with the controls, decreasing numbers of mitochondria (Fig. 2A and 2B, $P < 0.0001$ by unpaired *t*-test) and swollen mitochondria (Fig. 2C and 2D, $P < 0.0001$ by unpaired *t*-test) were found on TEM. Considering the TEM results showed morphological alteration in the mitochondria, putative functional alteration in the mitochondria was further detected among the patients. The patients had lower expression levels of ND1 at protein (Fig. 3C and 3D, $P = 0.0465$ by unpaired *t*-test) and mRNA levels (Fig. 3E, $P = 0.0331$ by unpaired *t*-test) than the controls. However, the expression of TRMT2B seemed unchanged between the patients and the controls (Fig. 3A and 3B). The activity of mitochondrial complexes I and III in lymphoblastoid cells was also examined from the two patients and the controls. The activities of complex I in the patients were lower than those in the other tested individuals ($P = 0.0251$ by unpaired *t*-test), including the carrier mother ($P= 0.0356$ by unpaired *t*-test). Although no significant difference was found among the three controls (carrier mother, healthy sister, and the unrelated man), the average value of the carrier mother was lower than that of the other controls. Meanwhile, no significant differences were observed in the activities of complex III (Figs. 3F and S5). The level of ROS in the lymphoblastoid cells of the patients also increased (Figs. 3G and S6; $P < 0.0001$ by unpaired *t*-test).

TRMT2B contribution to maintaining mitochondrial function

Two *TRMT2B*-interfering HEK293 cell lines were constructed using lentivirus to further explore the function of *TRMT2B* (Fig. S7A). A reduced number of mitochondria (Fig. 4A and 4B) and swollen mitochondria (Fig. 4C and 4D) were observed in the *TRMT2B*-interfering cell lines.

By interfering with the expression of *TRMT2B* in HEK293, the expression of ND1 decreased (Fig. 5A and 5B) in patients with *TRMT2B* variations. Further, no alteration was detected in the expression of MTCO1, MTCO2, or TFAM (Fig. 5C). By overexpression of *TRMT2B* and *TRMT2B* mutated proteins in HEK293, a

Table 3 Variations identified within patients with ALS

Sample ID	Sex	Age of onset	Gene	Chr	Position	Location	cDNA change	AA alteration	Mutation type	rsID	MAF in gnomAD	*P* value [b]	Functional predictions: pathogenic (total) [c]	Sequencing depth
XY003.P1 [a]	M	1	*TRMT2B*	X	100273992	Exon12	c.1356G>T	p.K452N	missense	/	/	/	2/11	79
XY003.P2 [a]	M	1	*TRMT2B*	X	100273992	Exon12	c.1356G>T	p.K452N	missense	/	/	/	2/11	86
M6783	M	66	*TRMT2B*	X	100296359	Exon3	c.250C>G	p.L84V	missense	rs201296426	0.0006019 (119/197698)	< 0.0001	5/11	9
M7966	F	63	*TRMT2B*	X	100296359	Exon3	c.250C>G	p.L84V	missense	rs201296426	0.0006019 (119/197698)	< 0.0001	5/11	8
S001433	F	65	*TRMT2B*	X	100296359	Exon3	c.250C>G	p.L84V	missense	rs201296426	0.0006019 (119/197698)	< 0.0001	5/11	17
S003418	F	42	*TRMT2B*	X	100296359	Exon3	c.250C>G	p.L84V	missense	rs201296426	0.0006019 (119/197698)	< 0.0001	5/11	11
S003943	M	50	*TRMT2B*	X	100296359	Exon3	c.250C>G	p.L84V	missense	rs201296426	0.0006019 (119/197698)	< 0.0001	5/11	16
S004576	M	56	*TRMT2B*	X	100296359	Exon3	c.250C>G	p.L84V	missense	rs201296426	0.0006019 (119/197698)	< 0.0001	5/11	5
S004913	M	50	*TRMT2B*	X	100296359	Exon3	c.250C>G	p.L84V	missense	rs201296426	0.0006019 (119/197698)	< 0.0001	5/11	8
M36116	F	58	*TRMT2B*	X	100290675	Exon7	c.539-3T>C	/	splicing	/	/		/	39
S003640	M	65	*TRMT2B*	X	100274004	Exon12	c.1344T>G	p.F448L	missense	rs374183741	0.00007793 (16/205319)	0.0961	6/11	61
/[d]	F	/	*TRMT2B*	X	100276156	Exon9	c.1000C>T	p.R334W	missense	rs145089500	0.00001637 (3/183278)	/	6/11	/
/[d]	/	/	*TRMT2B*	X	100276212	Exon9	c.944G>T	p.R315L	missense	rs145912589	0.0001268 (26/205046)	/	4/11	/
/[d]	/	/	*TRMT2B*	X	100292017	Exon5	c.484C>G	p.R162G	missense	rs141694732	0.00002923 (6/205301)	/	3/11	/

[a] Patients identified in a juvenile ALS family. [b] Comparing with whole population allele frequency in gnomAD. [c] The silico tools for predicting variants were (1) PolyPhen2 HDIV (polymorphism phenotyping version 2 human diversity), (2) PolyPhen2 HVAR (polymorphism pheno typing version 2 human variation), (3) SIFT (sorting intolerant from tolerant), (4) PROVEAN (protein variation effect analyzer), (5) GERP ++ (genomic evolutionary rate profiling), (6) CADD (combined annotation dependent depletion), (7) LRT (likelihood ratio test), (8) FATHMM (functional analysis through hidden Markov models), (9) M-CAP (Mendelian clinically applicable pathogenicity), (10) MutationTaster, and (11) MutationAssessor. [d] Data extracted from ALSdb.

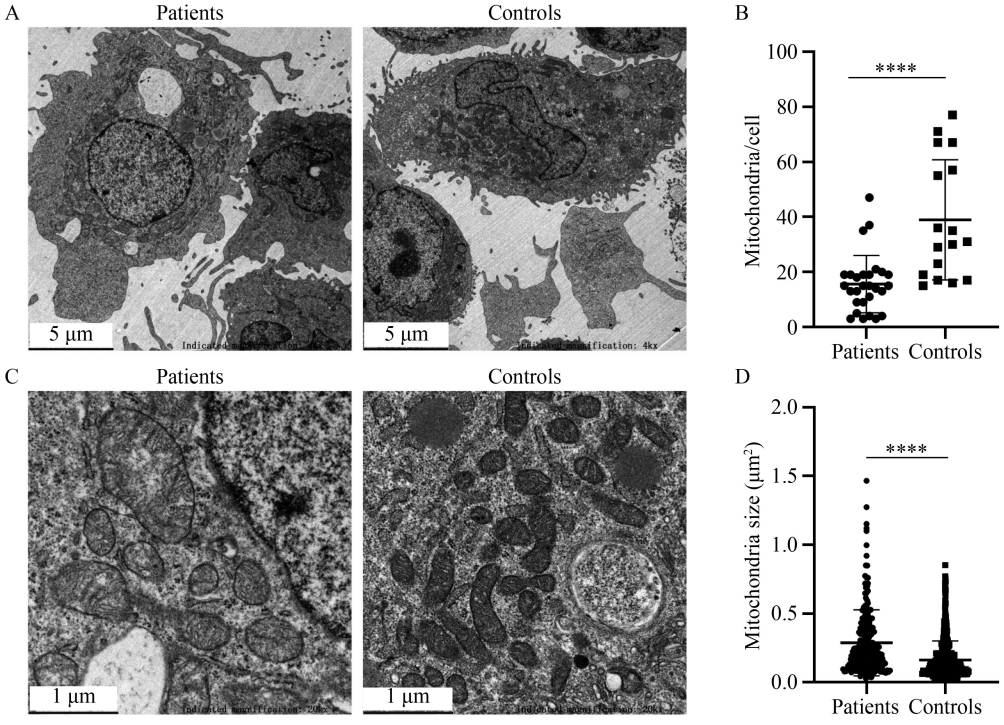

Fig. 2 Altered mitochondrial morphology in patients' lymphoblastoid cells. (A) TEM images showing reduced numbers of mitochondria in patients. (B) TEM images of lymphoblastoid cells from XY003.P1 (N = 13), XY003.P2 (N = 15), XY003.S1 (N = 7), and unrelated control (N = 10). (C) TEM images showing swollen mitochondria in patients. (D) TEM images of mitochondria from XY003.P1 (N = 120), XY003.P2 (N = 100), XY003.S1 (N = 185), and unrelated control (N = 274). The size of mitochondria in patients increased. **** $P < 0.0001$.

the lower expression of ND1 was found in the mutated groups (Fig. 5D and 5E). Compared with those in NC, the basal respiration, ATP production, maximal respiration, and spare respiratory capacity in the two *TRMT2B*-interfering HEK293 cell lines decreased according to the Seahorse XF Pro Analyzer, which indicated decreasing mitochondrial aerobic respiration induced by the down-expression of TRMT2B (Fig. S8A–S8G). Increased ROS levels were also detected in patients (Figs. 5F and S7B).

Immunocytochemistry analysis of HEK293 cells indicated that *TRMT2B* was co-localized with the mitochondrial marker TOMM20, and the mutated TRMT2B proteins were also located within the mitochondria (Fig. S9).

Thus, *TRMT2B* may play an important role in maintaining normal mitochondrial function.

Discussion

In this study, a novel ALS-associated gene called *TRMT2B* was identified by analyzing patients with familial and sporadic ALS. The proband of the family exhibited progressive muscular weakness and atrophy, cognitive impairment, and deformities in all four extremities, as well as impaired vision. The neurological examination revealed signs of upper and lower motor neuron lesions. The neurological electrophysiology analysis showed extensive chronic and ongoing neurogenic damage, indicating damage to the anterior horn cells in the spinal cord and pyramidal tract. After other neurological diseases were ruled out, the patient was diagnosed with fALS and ALS-Plus syndrome in accordance with the revised El Escorial criteria from 2000 [20,26]. ALS-Plus is used to classify patients with ALS who exhibit non-motor symptoms, such as oculomotor disorders, sensory disturbances, and cerebellar and extrapyramidal disorders [26,27].

In this study, other diseases were excluded from the differential diagnosis. Multisystem proteinopathy (MSP) is a pleiotropic degenerative disorder characterized by a combination of at least two of the following: body myopathy, Paget disease of the bone, and ALS/frontotemporal dementia [28]. Several ALS causative genes, such as *VCP*, *SQSTM1*, *HNRNPA2B1*, *HNRNPA1*, and *MATR3,* have been identified to be correlated with MSP phenotypes [28]. In the present study, MSP was also a possibility given the bone deformity and motor neuron dysfunction in the proband. However, on the basis of the phenotypes and ECG results of the patients, they were diagnosed with ALS-Plus. In addition, spinal muscular atrophy (SMA)-Plus and mitochondrial encephalomyopathy were not the appropriate diagnoses. The UMN signs did not support a diagnosis of SMA-Plus [29], and mitochondrial encephalomyopathy was ruled out because

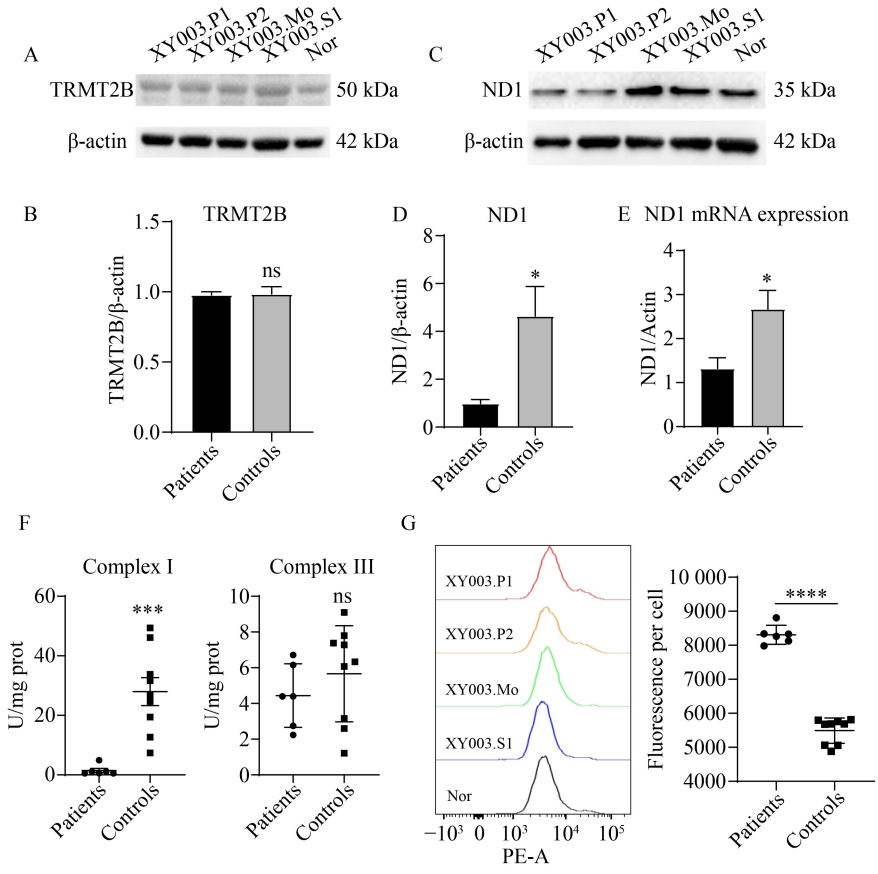

Fig. 3 Altered mitochondrial function in patients' lymphoblastoid cells. (A) Unchanged TRMT2B expression in patients. (B) Gray density analysis of TRMT2B. (C) Lower protein expression of ND1 in patients. (D) Gray density analysis of ND1 expression. (E) Lower mRNA expression of ND1 in patient-originated lymphoblastoid cells. (F) Decreased complex I activity in patients. (G) Increased ROS levels in patients. * $P < 0.05$, ** $P < 0.01$, *** $P < 0.001$, and **** $P < 0.0001$ by unpaired *t*-test.

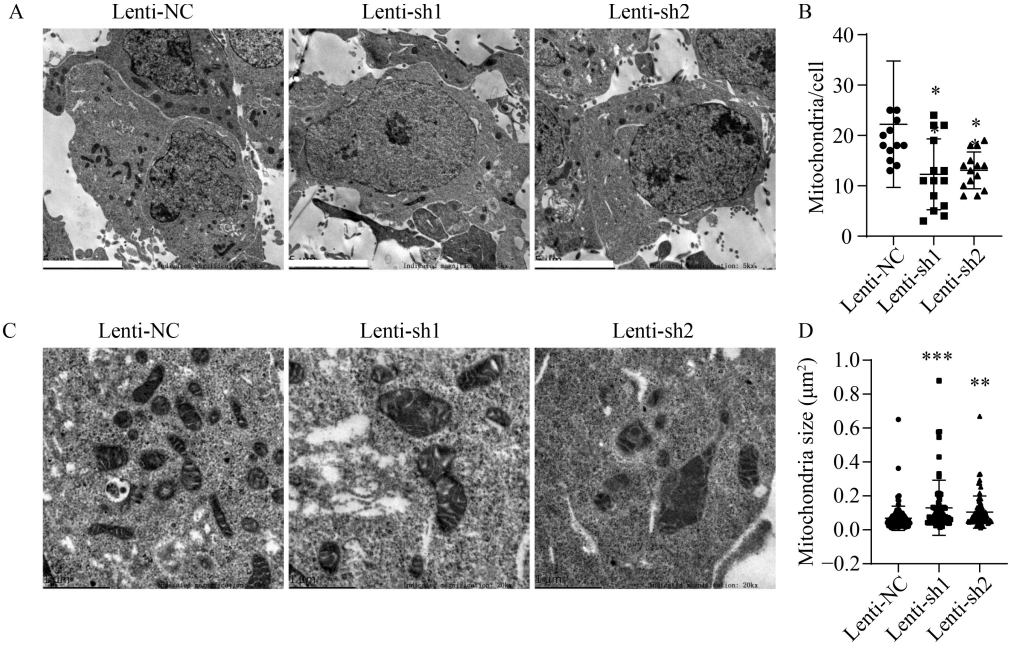

Fig. 4 Altered mitochondrial morphology in *TRMT2B*-interfering HEK293 lines. (A) and (B) Decreased number of mitochondria within *TRMT2B*-interfering HEK293 cells ($N_{NC} = 13$, $N_{sh} = 14$). (C,D) Swollen mitochondria within *TRMT2B*-interfering HEK293 cells ($N_{NC} = 120$, $N_{sh1} = 84$, $N_{sh2} = 79$). * $P < 0.05$, ** $P < 0.01$, and *** $P < 0.001$ by unpaired *t*-test.

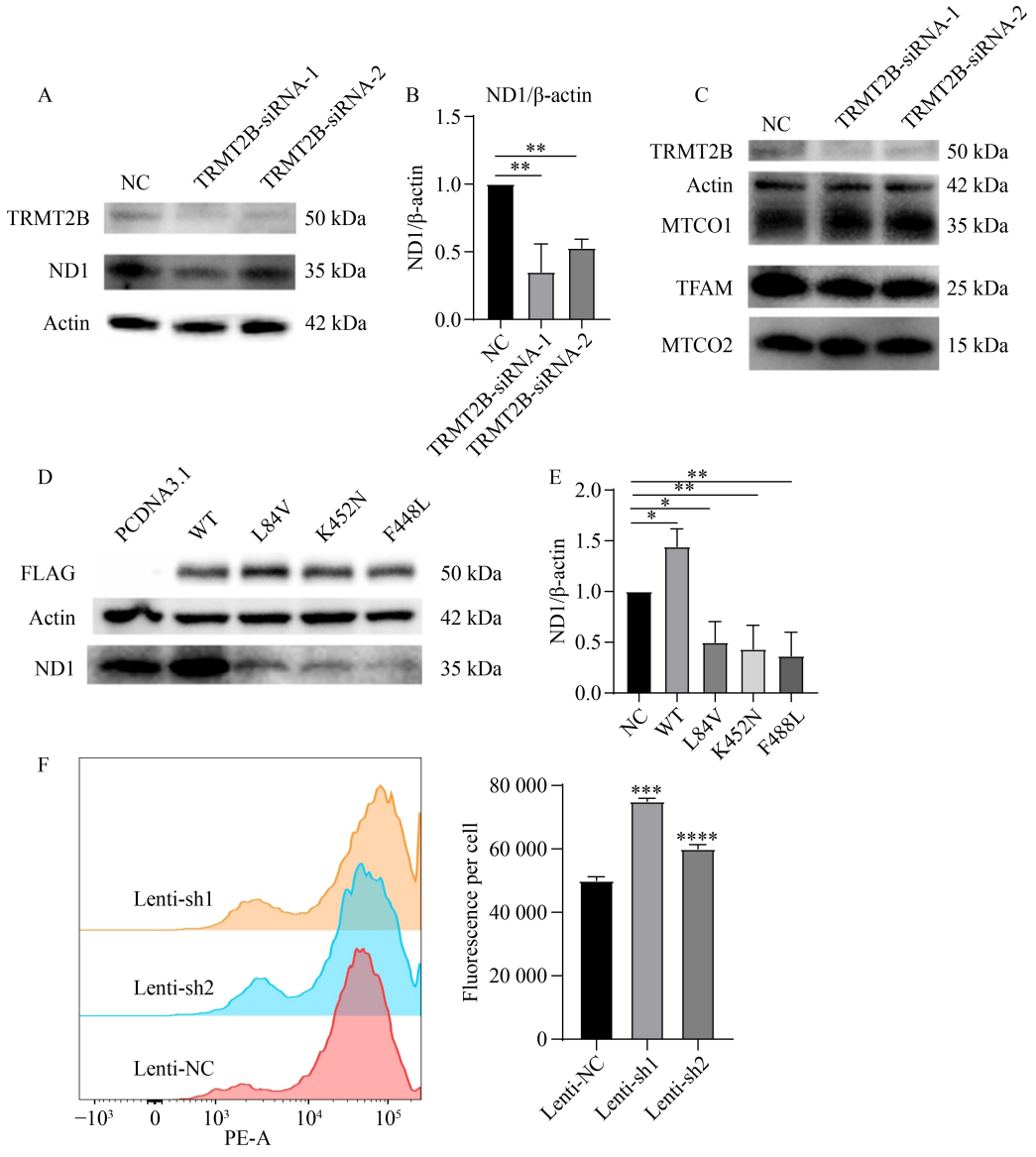

Fig. 5 Altered mitochondrial function in *TRMT2B*-interfering HEK293 lines. (A) Decreased ND1 expression by inhibition of TRMT2B expression. (B) Gray density analysis of ND1. (C) Unchanged expression of MTCO1, MTCO2, and TFAM when TRMT2B was interfered. (D) Decreased expression of ND1 in TRMT2B mutated overexpression groups. (E) Gray density analysis of WB lanes of ND1. (F) Increased ROS levels in *TRMT2B*-interfering HEK293 cells. * $P < 0.05$, ** $P < 0.01$, *** $P < 0.001$, and **** $P < 0.0001$ by unpaired *t*-test.

of the un-elevated level of lactate, the electrophysiological chronic and ongoing neurogenic changes instead of myogenic changes, and the normal brain MRI. Therefore, ALS-Plus was the more appropriate diagnosis, which may extend the phenotypic spectrum of the ALS-Plus syndrome.

TRMT2B is a gene located on the X chromosome that encodes tRNA methyltransferase 2 homolog B. Although the function of TRMT2B is not fully understood, it is believed to be responsible for the m^5U methylation in mitochondrial tRNA and rRNA, which is crucial for tRNA stability and maturation [30]. Inactivation of *TRMT2B* has been shown to decrease the activity of respiratory chain complexes I, III, and IV [31]. While one study suggested that *TRMT2B* may not be essential in human cells [32], dysregulation of tRNA post-transcriptional methylation has been linked to neural developments [33] and neurodegenerative diseases [30]. Other members of the TRMT gene family, such as *TRMT61B* [34], *TRMT1*, and *TRMT10A* [35,36], were supported to contribute to the pathogenesis of neurological disorders, such as AD and intellectual disability. Meanwhile, a previous study indicated that mice with a mutated *Trmt2b* exhibited abnormal physical strength [37]. These findings and the screening results of TRMT2B in the cohort may provide independent, albeit limited, evidence for the pathogenicity of *TRMT2B* in ALS.

Some ALS-associated genes, including *TARDBP*, *C9ORF72*, and *SOD1*, have been reported to play a role in the etiology of ALS by causing mitochondrial dysfunction [38–40]. An increasing body of research data suggested that imbalanced ROS plays a remarkable role in the onset and progression of various neurodegenerative disorders, such as ALS, AD, and PD [41]. Herein, in the patients' lymphocytes and *TRMT2B*-interfering cell lines, mitochondrial morphology alteration, reduced ND1 expression, lower mitochondrial complex I activity, decreased mitochondrial aerobic respiration, and increased ROS levels were observed, indicating mitochondrial dysfunction induced by TRMT2B loss of function.

TA cloning and sequencing showed that only 8.5% of the TRMT2B mRNA in the unaffected carrier mother had the c.1356G > T substitution, suggesting that the majority of the protein could be unaffected. The mitochondrial complex I activity in the carrier mother was normal and higher than that in patients, although the average value was lower than that in other normal controls, similar to the ROS level (Fig. S6). These results indicated that the accumulative effect of the lower activity did not reach the threshold for ALS onset. Consequently, the *TRMT2B* functional alterations identified in patients with ALS, especially women, may contribute to pathogenesis through dose- and time-dependent accumulation.

Due to technical limitations, mitochondrial tRNA methylation could not be directly examined using isotope labeling of tRNA. Alternative methods should be utilized in future studies. In addition, the lack of lymphoblastoid cell lines prevented the examination of mitochondrial complex activity and ROS production in patients with sporadic ALS with mutated *TRMT2B*. Future studies could concentrate on investigating the functions of mutated *TRMT2B* and validating accumulated effects.

In conclusion, a novel JALS-associated gene called *TRMT2B* was identified, which may contribute to the pathogenesis of ALS through the impairment of mitochondrial function.

Acknowledgements

The authors wish to thank the patients and their families for their participation in this project. This work was supported by the Program of the National Natural Science Foundation of China (Nos. 82171431 and 31972886), the Natural Science Fund for Distinguished Young Scholars of Hunan Province, China (Nos. 2020JJ2057 and 2021JJ10074), Natural Science Foundation of Changsha City (No. kq2208402), the Program of the National Natural Science Foundation of Hunan Province (No. 2021JJ40989), the Project Program of National Clinical Research Center for Geriatric Disorders at Xiangya Hospital (No. 2020LNJJ13), the Science and Technology Innovation 2030 (STI2030-Major Projects, No. 2021ZD0201803), the National Key R&D Program of China (No. 2021YFA0805202) the Innovation Team Project of Hunan Province (No. 2019RS1010), and the Innovation Team Project of Central South University (No. 2020CX016).

Compliance with ethics guidelines

Conflicts of interest Yanling Liu, Xi He, Yanchun Yuan, Bin Li, Zhen Liu, Wanzhen Li, Kaixuan Li, Shuo Tan, Quan Zhu, Zhengyan Tang, Feng Han, Ziqiang Wu, Lu Shen, Hong Jiang, Beisha Tang, Jian Qiu, Zhengmao Hu, and Junling Wang declare that they have no conflict of interest.

This study was approved by the Ethics Committee of Xiangya Hospital, Central South University, China. The approved number is 202103191. The study was performed in accordance with the ethical standards as laid down in the 1964 *Declaration of Helsinki* and its later amendments or comparable ethical standards. All participants provided written informed consent to the study. The authors affirm that human research participants provided informed consent for the publication of the images in Fig. 1D and Fig. S1.

Electronic Supplementary Material Supplementary material is available in the online version of this article at https://doi.org/10.1007/s11684-023-1005-y and is accessible for authorized users.

References

1. van Es MA, Hardiman O, Chio A, Al-Chalabi A, Pasterkamp RJ, Veldink JH, van den Berg LH. Amyotrophic lateral sclerosis. Lancet 2017; 390(10107): 2084–2098
2. Longinetti E, Fang F. Epidemiology of amyotrophic lateral sclerosis: an update of recent literature. Curr Opin Neurol 2019; 32(5): 771–776
3. Chia R, Chiò A, Traynor BJ. Novel genes associated with amyotrophic lateral sclerosis: diagnostic and clinical implications. Lancet Neurol 2018; 17(1): 94–102
4. Oskarsson B, Horton DK, Mitsumoto H. Potential environmental factors in amyotrophic lateral sclerosis. Neurol Clin 2015; 33(4): 877–888
5. Talbott EO, Malek AM, Lacomis D. The epidemiology of amyotrophic lateral sclerosis. Handb Clin Neurol 2016; 138: 225–238
6. Hou L, Jiao B, Xiao T, Zhou L, Zhou Z, Du J, Yan X, Wang J, Tang B, Shen L. Screening of SOD1, FUS and TARDBP genes in patients with amyotrophic lateral sclerosis in central-southern China. Sci Rep 2016; 6(1): 32478
7. Liu Z, Yuan Y, Wang M, Ni J, Li W, Huang L, Hu Y, Liu P, Hou X, Hou X, Du J, Weng L, Zhang R, Niu Q, Tang J, Jiang H, Shen L, Tang B, Wang J. Mutation spectrum of amyotrophic lateral sclerosis in Central South China. Neurobiol Aging 2021; 107: 181–188
8. Orban P, Devon RS, Hayden MR, Leavitt BR. Chapter 15 Juvenile amyotrophic lateral sclerosis. Handb Clin Neurol 2007; 82: 301–312
9. Johnson JO, Chia R, Miller DE, Li R, Kumaran R, Abramzon Y,

Alahmady N, Renton AE, Topp SD, Gibbs JR, Cookson MR, Sabir MS, Dalgard CL, Troakes C, Jones AR, Shatunov A, Iacoangeli A, Al Khleifat A, Ticozzi N, Silani V, Gellera C, Blair IP, Dobson-Stone C, Kwok JB, Bonkowski ES, Palvadeau R, Tienari PJ, Morrison KE, Shaw PJ, Al-Chalabi A, Brown RH Jr, Calvo A, Mora G, Al-Saif H, Gotkine M, Leigh F, Chang IJ, Perlman SJ, Glass I, Scott AI, Shaw CE, Basak AN, Landers JE, Chiò A, Crawford TO, Smith BN, Traynor BJ; FALS Sequencing Consortium; American Genome Center; International ALS Genomics Consortium; and ITALSGEN Consortium; et al. Association of variants in the SPTLC1 gene with juvenile amyotrophic lateral sclerosis. JAMA Neurol 2021; 78(10): 1236–1248

10. Lanteri P, Meola I, Canosa A, De Marco G, Lomartire A, Rinaudo MT, Albamonte E, Sansone VA, Lunetta C, Manera U, Vasta R, Moglia C, Calvo A, Origone P, Chiò A, Mandich P. The heterozygous deletion c.1509_1510delAG in exon 14 of FUS causes an aggressive childhood-onset ALS with cognitive impairment. Neurobiol Aging 2021; 103: 130.e1–130.e7
11. Sprute R, Jergas H, Ölmez A, Alawbathani S, Karasoy H, Dafsari HS, Becker K, Daimagüler HS, Nürnberg P, Muntoni F, Topaloglu H, Uyanik G, Cirak S. Genotype-phenotype correlation in seven motor neuron disease families with novel ALS2 mutations. Am J Med Genet A 2021; 185(2): 344–354
12. Chen YZ, Bennett CL, Huynh HM, Blair IP, Puls I, Irobi J, Dierick I, Abel A, Kennerson ML, Rabin BA, Nicholson GA, Auer-Grumbach M, Wagner K, De Jonghe P, Griffin JW, Fischbeck KH, Timmerman V, Cornblath DR, Chance PF. DNA/RNA helicase gene mutations in a form of juvenile amyotrophic lateral sclerosis (ALS4). Am J Hum Genet 2004; 74(6): 1128–1135
13. Orlacchio A, Babalini C, Borreca A, Patrono C, Massa R, Basaran S, Munhoz RP, Rogaeva EA, St George-Hyslop PH, Bernardi G, Kawarai T. SPATACSIN mutations cause autosomal recessive juvenile amyotrophic lateral sclerosis. Brain 2010; 133(2): 591–598
14. Al-Saif A, Al-Mohanna F, Bohlega S. A mutation in sigma-1 receptor causes juvenile amyotrophic lateral sclerosis. Ann Neurol 2011; 70(6): 913–919
15. Altman T, Ionescu A, Ibraheem A, Priesmann D, Gradus-Pery T, Farberov L, Alexandra G, Shelestovich N, Dafinca R, Shomron N, Rage F, Talbot K, Ward ME, Dori A, Krüger M, Perlson E. Axonal TDP-43 condensates drive neuromuscular junction disruption through inhibition of local synthesis of nuclear encoded mitochondrial proteins. Nat Commun 2021; 12(1): 6914
16. Anoar S, Woodling NS, Niccoli T. Mitochondria dysfunction in frontotemporal dementia/amyotrophic lateral sclerosis: lessons from *Drosophila* models. Front Neurosci 2021; 15: 786076
17. Theunissen F, West PK, Brennan S, Petrović B, Hooshmand K, Akkari PA, Keon M, Guennewig B. New perspectives on cytoskeletal dysregulation and mitochondrial mislocalization in amyotrophic lateral sclerosis. Transl Neurodegener 2021; 10(1): 46
18. Martin LJ. Mitochondriopathy in Parkinson disease and amyotrophic lateral sclerosis. J Neuropathol Exp Neurol 2006; 65(12): 1103–1110
19. Wang T, Liu H, Itoh K, Oh S, Zhao L, Murata D, Sesaki H, Hartung T, Na CH, Wang J. C9orf72 regulates energy homeostasis by stabilizing mitochondrial complex I assembly. Cell Metab 2021; 33(3): 531–546.e9
20. Ludolph A, Drory V, Hardiman O, Nakano I, Ravits J, Robberecht W, Shefner J; WFN Research Group On ALS/MND. A revision of the El Escorial criteria—2015. Amyotrop Lat Scl Fr Deg 2015; 16(5–6): 291–292
21. Jiang X, Teng Y, Chen X, Liang N, Li Z, Liang D, Wu L. Six novel mutation analysis of the androgen receptor gene in 17 Chinese patients with androgen insensitivity syndrome. Clin Chim Acta 2020; 506: 180–186
22. Guo H, Tong P, Liu Y, Xia L, Wang T, Tian Q, Li Y, Hu Y, Zheng Y, Jin X, Li Y, Xiong W, Tang B, Feng Y, Li J, Pan Q, Hu Z, Xia K. Mutations of P4HA2 encoding prolyl 4-hydroxylase 2 are associated with nonsyndromic high myopia. Genet Med 2015; 17(4): 300–306
23. Tian Y, Wang JL, Huang W, Zeng S, Jiao B, Liu Z, Chen Z, Li Y, Wang Y, Min HX, Wang XJ, You Y, Zhang RX, Chen XY, Yi F, Zhou YF, Long HY, Zhou CJ, Hou X, Wang JP, Xie B, Liang F, Yang ZY, Sun QY, Allen EG, Shafik AM, Kong HE, Guo JF, Yan XX, Hu ZM, Xia K, Jiang H, Xu HW, Duan RH, Jin P, Tang BS, Shen L. Expansion of human-specific GGC repeat in neuronal intranuclear inclusion disease-related disorders. Am J Hum Genet 2019; 105(1): 166–176
24. He X, Huang Z, Liu W, Liu Y, Qian H, Lei T, Hua L, Hu Y, Zhang Y, Lei P. Electrospun polycaprolactone/hydroxyapatite/ZnO films as potential biomaterials for application in bone-tendon interface repair. Coll Surf B Bioint 2021; 204: 111825
25. Grieco JP, Compton SLE, Bano N, Brookover L, Nichenko AS, Drake JC, Schmelz EM. Mitochondrial plasticity supports proliferative outgrowth and invasion of ovarian cancer spheroids during adhesion. Front Oncol 2023; 12: 1043670
26. Brooks BR, Miller RG, Swash M, Munsat TL; World Federation of Neurology Research Group on Motor Neuron Diseases. El Escorial revisited: revised criteria for the diagnosis of amyotrophic lateral sclerosis. Amyotrop Lat Scl Oth Mot Neur Dis 2000; 1(5): 293–299
27. McCombe PA, Wray NR, Henderson RD. Extra-motor abnormalities in amyotrophic lateral sclerosis: another layer of heterogeneity. Expert Rev Neurother 2017; 17(6): 561–577
28. Taylor JP. Multisystem proteinopathy: intersecting genetics in muscle, bone, and brain degeneration. Neurology 2015; 85(8): 658–660
29. Teoh HL, Carey K, Sampaio H, Mowat D, Roscioli T, Farrar M. Inherited paediatric motor neuron disorders: beyond spinal muscular atrophy. Neural Plast 2017; 2017: 6509493
30. Pereira M, Francisco S, Varanda AS, Santos M, Santos MAS, Soares AR. Impact of tRNA modifications and tRNA-modifying enzymes on proteostasis and human disease. Int J Mol Sci 2018; 19(12): 3738
31. Laptev I, Shvetsova E, Levitskii S, Serebryakova M, Rubtsova M, Bogdanov A, Kamenski P, Sergiev P, Dontsova O. Mouse Trmt2B protein is a dual specific mitochondrial metyltransferase responsible for m^5U formation in both tRNA and rRNA. RNA Biol 2020; 17(4): 441–450
32. Powell CA, Minczuk M. TRMT2B is responsible for both tRNA and rRNA m^5U-methylation in human mitochondria. RNA Biol 2020; 17(4): 451–462
33. Zhang F, Yoon K, Zhang DY, Kim NS, Ming GL, Song H. Epitranscriptomic regulation of cortical neurogenesis via Mettl8-dependent mitochondrial tRNA m^3C modification. Cell Stem Cell

2023; 30(3): 300–311.e11

34. Sekar S, McDonald J, Cuyugan L, Aldrich J, Kurdoglu A, Adkins J, Serrano G, Beach TG, Craig DW, Valla J, Reiman EM, Liang WS. Alzheimer's disease is associated with altered expression of genes involved in immune response and mitochondrial processes in astrocytes. Neurobiol Aging 2015; 36(2): 583–591
35. Davarniya B, Hu H, Kahrizi K, Musante L, Fattahi Z, Hosseini M, Maqsoud F, Farajollahi R, Wienker TF, Ropers HH, Najmabadi H. The role of a novel TRMT1 gene mutation and rare GRM1 gene defect in intellectual disability in two Azeri families. PLoS One 2015; 10(8): e0129631
36. Igoillo-Esteve M, Genin A, Lambert N, Désir J, Pirson I, Abdulkarim B, Simonis N, Drielsma A, Marselli L, Marchetti P, Vanderhaeghen P, Eizirik DL, Wuyts W, Julier C, Chakera AJ, Ellard S, Hattersley AT, Abramowicz M, Cnop M. tRNA methyltransferase homolog gene TRMT10A mutation in young onset diabetes and primary microcephaly in humans. PLoS Genet 2013; 9(10): e1003888
37. Koscielny G, Yaikhom G, Iyer V, Meehan TF, Morgan H, Atienza-Herrero J, Blake A, Chen CK, Easty R, Di Fenza A, Fiegel T, Grifiths M, Horne A, Karp NA, Kurbatova N, Mason JC, Matthews P, Oakley DJ, Qazi A, Regnart J, Retha A, Santos LA, Sneddon DJ, Warren J, Westerberg H, Wilson RJ, Melvin DG, Smedley D, Brown SD, Flicek P, Skarnes WC, Mallon AM, Parkinson H. The International Mouse Phenotyping Consortium Web Portal, a unified point of access for knockout mice and related phenotyping data. Nucleic Acids Res 2014; 42(Database issue): D802–D809
38. De Vos KJ, Chapman AL, Tennant ME, Manser C, Tudor EL, Lau KF, Brownlees J, Ackerley S, Shaw PJ, McLoughlin DM, Shaw CE, Leigh PN, Miller CCJ, Grierson AJ. Familial amyotrophic lateral sclerosis-linked SOD1 mutants perturb fast axonal transport to reduce axonal mitochondria content. Hum Mol Genet 2007; 16(22): 2720–2728
39. Wang P, Deng J, Dong J, Liu J, Bigio EH, Mesulam M, Wang T, Sun L, Wang L, Lee AY, McGee WA, Chen X, Fushimi K, Zhu L, Wu JY. TDP-43 induces mitochondrial damage and activates the mitochondrial unfolded protein response. PLoS Genet 2019; 15(5): e1007947
40. Murphy MP. Mitochondrial dysfunction indirectly elevates ROS production by the endoplasmic reticulum. Cell Metab 2013; 18(2): 145–146
41. Sivandzade F, Prasad S, Bhalerao A, Cucullo L. NRF2 and NF-κB interplay in cerebrovascular and neurodegenerative disorders: molecular mechanisms and possible therapeutic approaches. Redox Biol 2019; 21: 101059